K_a-Band 100-kW Subnanosecond Pulse Generator Mode-Locked by a Nonlinear Cyclotron Resonance Absorber

N. S. Ginzburg, S. V. Samsonov, G. G. Denisov, M. N. Vilkov, I. V. Zotova,* A. A. Bogdashov, I. G. Gachev, A. S. Sergeev, and R. M. Rozental

Institute of Applied Physics RAS, 603950, Nizhny Novgorod, Russia

(Received 6 July 2021; revised 4 October 2021; accepted 5 November 2021; published 24 November 2021)

We present the results of experiments on the generation of periodical trains of subnanosecond K_a-band pulses in the electron generator, which is based on passive mode locking. This technique is broadly used in laser physics for the generation of ultrashort pulses (USPs) but has not been previously employed in high-power microwave electronics. The microwave USP generator comprises a helical-waveguide gyrotron traveling wave tube and a saturable absorber in the feedback loop. Saturable absorption is implemented in an auxiliary section using the cyclotron resonance interaction with an initially rectilinear electron beam, for which nonlinear saturation is caused by the effect of the relativistic dependence of the gyrofrequency on the particle's energy. In agreement with theoretical predictions, periodical trains of 0.4-ns pulses with a peak power of 100 kW and repetition of 2.5 ns are measured. Phase coherence of radiated pulses is demonstrated based on analysis of the autocorrelation function. The experiments performed open a wide range of possibilities for the generation of coherent broadband radiation, which is in high demand for numerous applications.

DOI: 10.1103/PhysRevApplied.16.054045

I. INTRODUCTION

The development of high-power sources of pulsed microwave radiation [1–5] is of increasing interest for numerous scientific and technological applications, including diagnostics of dense plasmas, atmospheric sounding, and particle acceleration. An important point may be the phase correlation of generated pulses when the radiation spectrum is a so-called "frequency comb." In laser physics, there is a well-known principle for producing frequency combs based on the effect of passive mode locking [6–10], which is achieved by incorporating a saturable absorber (nonlinear filter) into the laser resonator. Actually, such an element acts as a nonlinear modulator of radiation losses. As a result, periodical trains of ultrashort (femtosecond) pulses of light can appear, which is widely used in lasers [8,9], including master generators of modern petawatt-laser facilities [10]. From a general point of view, the generated pulses are considered as dissipative solitons [11–13], the formation of which is due to the balance of amplification, absorption, harmonic generation, and group-velocity dispersion effects.

According to theoretical considerations, a similar method of ultrashort pulse (USP) generation can be realized in a two-section microwave generator consisting of an electronic amplifier and a nonlinear absorber in the feedback loop [14–17]. Such a scheme is quite universal, in the sense that an amplifier can be based on any known type of interaction [Cherenkov traveling wave tube (TWT), gyrotron TWT (gyro TWT), and so on], as long as it provides a sufficiently wide-gain bandwidth to effectively amplify short wide-spectrum pulses. At the same time, the critical issue for the development of mode-locked electron generators is the implementation of nonlinear absorbers that would be applicable to the microwave-frequency band and suitable for high-power operation. This problem was solved in Refs. [15,17], where we suggested several methods, including cyclotron resonance interaction of radiation with an initially rectilinear magnetized electron beam. As it is known, such a beam absorbs radiation under the conditions of the normal Doppler effect, which realizes when waves propagate in hollow waveguides. However, linear cyclotron resonance absorption is typically considered in numerous studies with the aim of cyclotron resonance plasma heating. At the same time, a saturation of absorption, in this case, is caused by the fundamental effect of the relativistic dependence of the gyrofrequency on the particle energy [18], which provides the required nonlinearity. As it is known from gyrotron theory, such a dependence may be significant, even for nonrelativistic energies of electrons.

This paper presents the results of experiments devoted to the practical implementation of a K_a-band electronic generator with mode locking by the cyclotron resonant absorber. A helical-waveguide gyro TWT [19–22] is used as an amplifying unit, providing a wide-gain band of up to

*zotova@appl.sci-nnov.ru

10%–15%, which is sufficient for effective amplification of generated microwave pulses with subnanosecond duration [23]. The experimental results are preceded by basic theoretical considerations, explaining the choice of the main parameters and results of numerical simulations within the frame of the averaged model previously developed in Ref. [17].

II. THEORETICAL BASIS

The principal scheme of the microwave mode-locked generator is presented in Fig. 1. The amplifying section (gyro TWT, Fig. 1, sec. 1) with a helically corrugated waveguide is powered by an axis-encircling electron beam, which excites the operating mode at the second-harmonic of the gyrofrequency, $s_1 = 2$. In the absorber (Fig. 1, sec. 2) with a regular cylindrical waveguide, an initially rectilinear electron beam interacts with the electromagnetic field at the fundamental cyclotron harmonic, $s_2 = 1$. The sections are coupled by a quasi-optical transmission line, which, in the developed time-domain model, is described by equivalent boundary conditions corresponding to a partially transparent mirror with power-reflection coefficient R and time delay T_d for a signal traveling between sections.

When using a helically corrugated waveguide, $r(\varphi, z) = r + \tilde{r}\cos(\bar{m}\varphi - \bar{h}z)$ (where r is the waveguide mean radius; $\tilde{r}$ and d are the corrugation amplitude and period, respectively; $\bar{m}$ is the number of corrugation folds; and $\bar{h} = 2\pi/d$), the resonant coupling of two counter-rotating $TE_{m,n}$ modes of an unperturbed cylindrical waveguide is provided [19]. One of these modes is a near-cutoff mode, A, with a small axial wave number, $h_A << k = \omega/c$, while

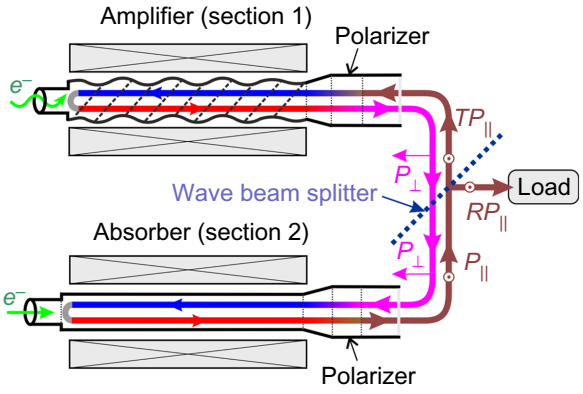

FIG. 1. (a) Principal scheme of a microwave mode-locked generator comprising a helical-waveguide gyro TWT (amplifier) and a regular-waveguide saturable cyclotron resonance absorber (blue and red arrows inside both tubes correspond to idle and active wave propagation, respectively); wave beam splitter is a quasi-optical system, enabling almost total transmission for one linear polarization, $P_\perp$ (purple line), and outcoupling of orthogonal polarization, $P_{||}$ (brown line), to the load with power-factor R.

the other partial wave, a far-from-cutoff traveling mode, B, has a large axial wave number, $h_B \sim k$. As a result, the operating normal wave, W, is formed, the dispersion characteristic, $\omega(h)$, of which is given by

$$[2\omega_A(\omega - \omega_A) - h^2c^2]\left[\frac{\omega_A(\omega - \omega_A)}{h_0c^2} - \bar{h} + h_0 - h\right] = \frac{2\sigma^2\omega_A^4}{h_0c^2}, \quad (1)$$

where $h_0 = h_B(\omega_A)$ is the wave number of mode B at cutoff frequency ω_A of mode A; σ is the coupling parameter proportional to the corrugation amplitude [19]. As shown in Ref. [23], in contrast with experimentally realized cw gyro TWTs [19–21], the maximum amplification of short electromagnetic pulses is achieved in the regime of intersection [see Fig. 2(a)] between the characteristic (1) and the beamline, $\omega = hV_{||1} + s_1\omega_{H1}$ (where $\omega_{H1} = eH_1/mc\gamma_1$ is the relativistic gyrofrequency, H_1 is the guiding magnetic field in the amplifying unit, and γ_1 is the Lorentz factor). In this case, since the group velocity of the normal wave differs from the axial electron velocity, $V_{||1}$, the microwave pulse "slips" over the electron beam and accumulates energy from different electron fractions. As a result, the output peak power of the pulse can significantly exceed the saturation level for the amplification of stationary monochromatic signals.

After the amplifier, the signal enters the absorber (Fig. 1, sec. 2), which has the form of a smoothly tapered regular waveguide driven by a magnetized, initially rectilinear (i.e., initially nonrotating), electron beam. Notably, similar to optics, the principal factor for efficient USP generation is the minimization of the absorber relaxation time. In laser physics, it can be satisfied, for example, by using Kerr lenses [7]. For the considered cyclotron absorber, this requirement means the minimization of the mutual influence between different parts of the microwave pulse through the electron beam. Such a condition is fulfilled when the operating-wave group velocity is close to the axial velocity of the electrons, $V_{||2}$. Actually, in this case, we have the local interaction (i.e., interaction without slippage) of every part of the microwave pulse with a corresponding fraction of the electron beam. This regime, which can be referred to as the group synchronism, corresponds to the grazing incidence between the beamline at the first cyclotron harmonic, $\omega = hV_{||2} + \omega_{H2}$, and the dispersion characteristic of the operating waveguide mode [see Fig. 2(b)].

The explanation provided makes it possible to roughly determine the main experimental parameters. Further optimization is carried out within the framework of the averaged model described in detail in Ref. [17]. The model includes self-consistent systems of nonstationary equations for each section and boundary conditions corresponding

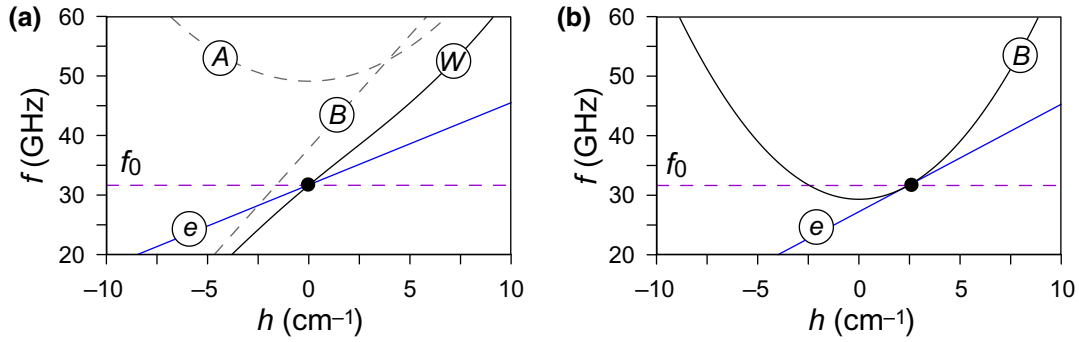

FIG. 2. Dispersion diagrams in amplifying (a) and absorbing (b) sections for the operating frequency $f_0 \approx 32$ GHz; A and B are dispersion characteristics of cutoff and traveling modes, respectively; W is the normal wave in the amplifying section. Beamlines are indicated by the letter e. $f = \omega/2\pi$.

to the scheme in Fig. 1. For comparison with experiments, we present the results of numerical simulations for selected parameters of amplifying and absorbing sections in Table I. The reflection coefficient, $R = 0.1$, and the delay time in the feedback loop, $T_d = 25$ ns, are also chosen to be close to experimental data.

The regime of periodical pulse generation obtained in the simulation is shown in Fig. 3(a). Electromagnetic pulses have a subnanosecond duration (about 300 ps FWHM) and a peak power of about 100 kW. The spectrum width is about 2–2.5 GHz [Fig. 3(b)] and, like the pulse duration, is determined by the amplification band. Similar to optics, the mechanism of pulse formation is associated with the effect of passive mode locking; thus, spectral lines correspond to eigenfrequencies of the feedback-loop modes. From a general point of view, the generated pulses can be considered as dissipative solitons [11–13]; this analogy is stated in Ref. [16].

In the considered case of rather–low absorption, generation develops from electron beam fluctuations (soft self-excitation regime). In such a regime, each microwave pulse occurs practically immediately after the previous one exits the amplifier. Thus, the distance between pulses of about 2 ns (repetition period T) approximately corresponds to the time of microwave-pulse slippage along the electron beam at amplifier length l_1. This value, which may be roughly estimated as $T \sim l_1(V_{||1}^{-1} - V_{\rm gr}^{-1})$, where $V_{\rm gr}$ is the group velocity of the normal wave, W, actually determines the distance between the main spectrum lines.

TABLE I. Main parameters of the experimentally realized K_a-band USP generator.

	Amplifier	Absorber
Electron energy	50 keV	40 keV
Electron current	6.7 A	1 A
Pitch factor	∼1	0
Interaction length	244 mm	91 mm
Waveguide radius	3.57 mm	2.96 mm
Corrugation period	11.6 mm	–
Corrugation amplitude	0.45 mm	–
Operating mode	$TE_{2,1}/TE_{1,1}$	$TE_{1,1}$
Magnetic field	∼0.65 T	∼1.1 T

III. EXPERIMENTAL SETUP AND RESULTS

Based on the theoretical analysis, the two-section K_a-band USP generator is developed, and an appropriate experimental setup (Fig. 4) is built.

The gyro TWT and the absorber tubes both use dc liquid-cooled solenoids and are powered through appropriate resistor dividers by one high-voltage pulsed modulator with about 100-μs flat-top (0.5%–1% variation) duration and up to 10-Hz pulse-repetition frequency. Thermionic cathodes used in both tubes are heated by individual power supplies, enabling control of the beam currents from 0 A to about 1.5 A in the absorber and up to 8 A in the amplifier. The gyro TWT assembly also includes a reverse dc cathode coil, the tuning of which enables precise and wide-range control of the electron pitch factor, $g = V_{\perp 1}/V_{||1}$, and, thus, the efficiency of the electron-wave interaction in the amplifier. The absorber gun, with a Pierce-type configuration, immersed in a converging magnetic field of an iron-shelled solenoid forms an almost rectilinear electron beam with a diameter of about 1.5 mm.

An external microwave circuit, ensuring the feedback loop shown in Fig. 1, is implemented in the form of the quasi-optical (QO) system shown schematically in Fig. 4(b). This circuit is based on principles developed in Ref. [24] for feeding and extracting power to and from the gyro TWT through one window. Both devices, the amplifier and absorber, use the cyclotron resonance interaction, which is polarization-dependent with respect to the left-handed or right-handed circularly polarized waves. This fact, together with the use of passive polarizers converting the linearly polarized wave into the circularly polarized one (and vice versa), ensures a situation

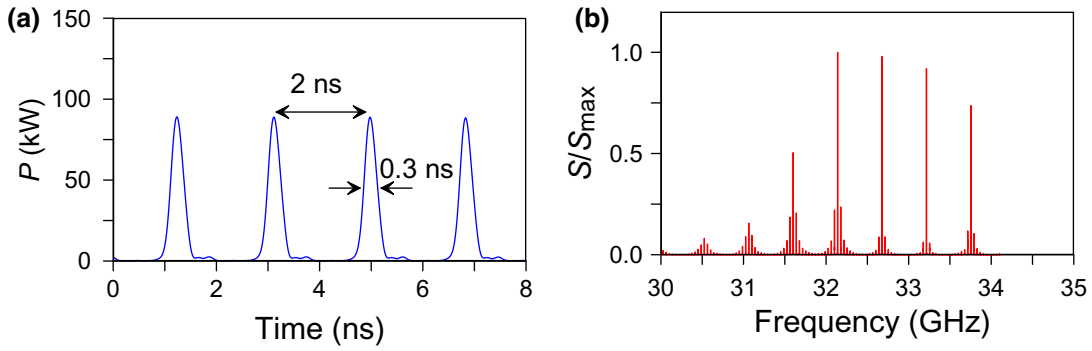

FIG. 3. Simulations of USP generation for experimental parameters. (a) Profile of microwave pulses; (b) radiation spectrum.

where the incoming wave with a certain linear polarization propagates the electron-beam flow upstream practically without any interaction. While propagating downstream (after being reflected by a subcutoff narrowing), the wave actively interacts with the electron beam (resulting in amplification or absorption) and leaves the tube through the same window in the form of a wave with the same transverse pattern but with orthogonal polarization, as shown in Fig. 1. For both tubes, just after, or before the polarizer, the wave has the form of the $TE_{1,1}$ circular-waveguide mode. To convert it into the Gaussian beam, a specially profiled taper with an output diameter of 63.5 mm is used for each tube.

In the experiments under discussion, the Gaussian beam leaving the amplifier has the rf electric field parallel to the x axis (x polarization) [Fig. 4(b)]. It is focused and successively directed by focusing mirrors MF1 and MF2, wire-grid $G1$, plane mirror MP, wire-grid $G2$, focusing mirrors MF3 and MF4 to the input-output port of the absorber. After interaction, the wave leaves the absorber in the form of a y-polarized Gaussian beam [blue ray in Fig. 4(b)]. This wave beam is focused and directed by mirrors MF4 and MF3, passes through wire-grid $G2$, and is reflected by mirror MC with sinusoidal corrugation, the orientation of which can be varied by mirror rotation around its axis, as shown in Fig. 4(b). Due to

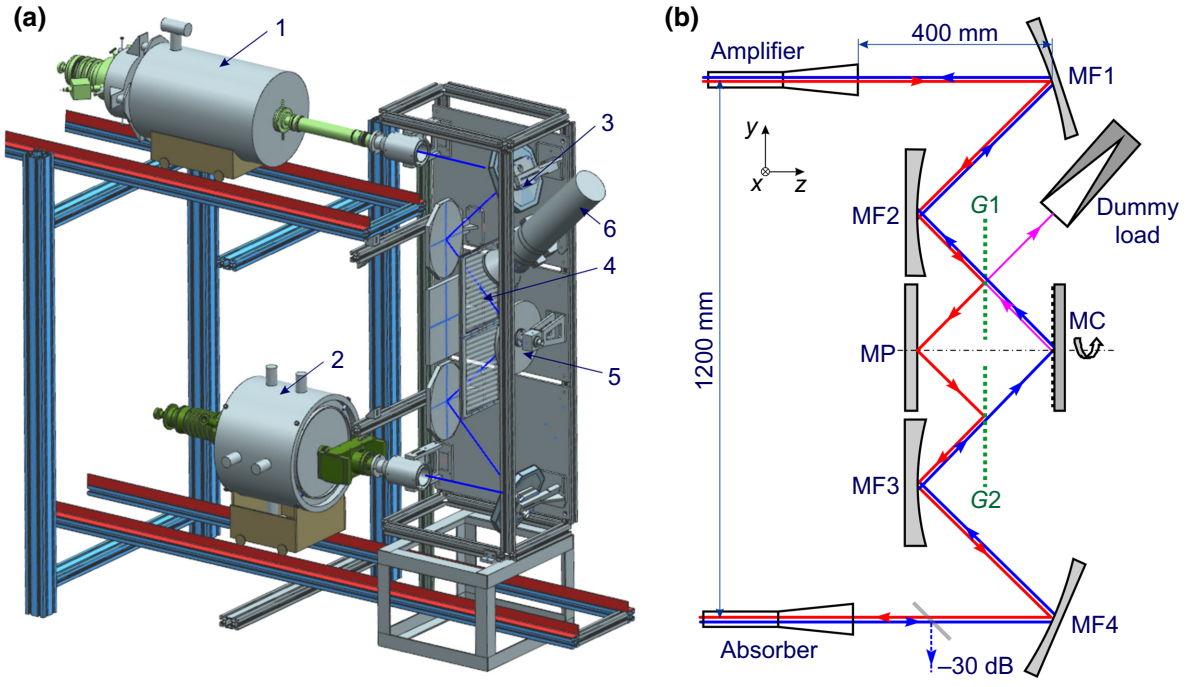

FIG. 4. Experimental setup of the K_a-band USP generator. (a) Three-dimensional visualization; (b) QO system scheme; 1, gyro TWT (amplifier); 2, cyclotron resonance absorber; 3, focusing mirror (MF1); 4, polarization splitter in the form of a grid of horizontal wires ($G1$); 5, rotating mirror with a corrugated surface (MC); 6, dummy load. Red (magenta) and blue arrows correspond to Gaussian-beam paths with mutually orthogonal linear polarizations; red and magenta are for x polarization.

corrugation, the x-polarized component occurs in the specularly reflected beam [magenta ray in Fig. 4(b)]. The relative power of this x-polarized beam, referred to in theory as R (see Fig. 1), can be varied from 0% to almost 100%, depending on the MC orientation angle. This beam is then reflected by wire-grid $G1$ to the dummy load, while the rest of the power is propagated in orthogonal polarization through $G1$ and is successively directed by MF2 and MF1 to the input-output of the amplifier in the form of a y-polarized beam.

Due to some imperfections of the elements and Ohmic loss (especially inside the tubes' interaction circuits), the total spurious losses of the circuit are quite high. The evaluation based on calculations and partial measurements gives a 30%–50% value for one-round-trip loss when R equals zero.

Before operation of the USP generator, the gyro TWT and the cyclotron absorber are individually tested using seed signals from a pulsed magnetron with a power of about 10 kW, pulse duration of 2 μs, and mechanically tunable frequency, resulting in reasonable agreement with the designed characteristics. The feedback QO system is cold-tested, aligned, and calibrated using a K_a-band scalar network analyzer. During the individual "hot" tests of the gyro TWT and the absorber, some system elements, namely, mirrors MF1 and MF4 [see Fig. 4(b)], are also aligned when the microwave-beam patterns are visualized using a neon-bulb discharging panel or replaceable sheets of thermosensitive paper.

To monitor the microwave signal circulating within the USP-generator circuit, a QO outcoupler is used in the form of a thin dielectric film deflecting about −30 dB of the Gaussian-beam output from the absorber [see Fig. 4(b)]. A small part (about −20 dB) of this deflected beam is picked up by the open end of a waveguide and delivered through a K_a-band rectangular-waveguide line to a rf-monitoring facility. This facility, along with some standard K_a-band components, such as attenuators, a directional coupler, a microwave diode detector, and a waveguide-to-coaxial adapter, include (for final measurements) a 59-GHz Keysight DSAZ594A oscilloscope that records both detected and nonrectified waveforms of the microwave signals. The absolute calibration of the detected signals with respect to the total Gaussian-beam power is performed in steady-state single-frequency oscillation regimes, with 100-μs pulses shooting at 10-Hz repetition frequency when the whole pulse power of about 30 kW is absorbed in the calorimetric dummy load. The accuracy of the peak-power measurements in the operating regime of USP generation can be estimated as ±10%.

In the hot experiments with the USP-generator configuration, a number of available electrical parameters (two dc solenoid currents, two cathode filament currents, the modulator voltage, gyro TWT cathode coil current), as well as the rotation angle of the corrugated mirror MC, are varied, with the aim of realizing stable trains of microwave pulses with the shortest duration and the highest peak power.

As a result of experimental optimization, a regime with the parameters presented in Table I is found, in which periodical trains of ultrashort (subnanosecond) and high-peak-power pulses are observed [Fig. 5(a)]. When the beam current in the absorber is set to zero, the system also generates periodical pulses in the regime of self-modulation, which is typical for amplifiers with delayed feedback. The average radiation power is practically the same in both, but the pulses are significantly longer, about 2.5 times lower in peak power, and not so reproducible [Fig. 5(b)]. The rf-monitoring equipment allows the pulse waveforms to be recorded with maximum resolution [Fig. 5(c)] for the time interval of 2 μs, during which the average power is quite stable, and all the pulses have a FWHM of (0.43 ± 0.03) ns and a repetition period of 2.57 ns. The level of maximum peak power (P_{max} in Fig. 5) corresponds to 100 kW. Notably, this value significantly exceeds the saturation level of the stationary amplification of 30 kW, which is achieved in the gyro TWT without the cyclotron absorber.

The evaluated spectrum of the 2-μs pulse train [Fig. 6(a)] is fairly reproducible from shot to shot. Its total width of nearly 2.5 GHz corresponds to the single-pulse duration, whereas the distance between the main lines of 0.39 GHz corresponds to the pulse repetition period. The measured width of each spectral line of about 0.5 MHz

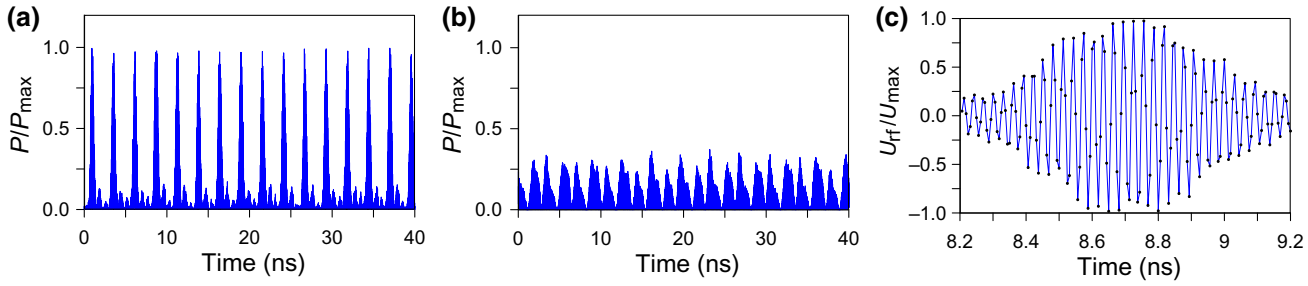

FIG. 5. Processed oscilloscope traces. Squared normalized rf signals recorded with 6.25-ps time step for the operating regime (a) and for the case when the absorber beam is switched off (b); profile of a typical single pulse in the operating regime (c).

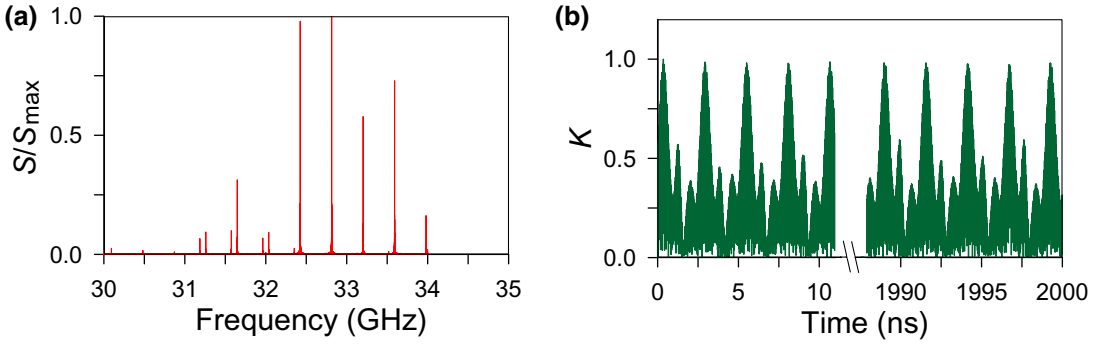

FIG. 6. (a) Fourier transform of the recorded USP train with 2 - μs duration. (b) Corresponding autocorrelation function.

is determined by the record duration of 2 μs. This narrow width of spectral lines, together with equal distances between them, provides the most evident verification of the very good coherence of the generated pulses, i.e., long-term stability of the frequency and the phase of oscillations. The latter fact is also confirmed by calculating the autocorrelation function [Fig. 6(b)] using the recorded rf-filled signal.

IV. CONCLUSION

Thus, in the experiments carried out, radiation with unique parameters is obtained in the two-section K_a-band generator driven by the helical-waveguide gyro TWT and mode-locked by the cyclotron resonance absorber. In general, the experiments demonstrate the principal feasibility of a class of microwave pulse generators realizable at various output-power levels and in various wavebands, making use of various types of wideband-electron amplifiers. The obtained 100-kW peak power of generated subnanosecond pulses significantly exceeds the mW level of microwave-frequency combs obtained previously based on semiconductor lasers with optoelectronic feedback [25]. With a further increase in frequency and power, mode-locked electronic generators may be in demand for modern methods of particle acceleration (cf. Ref. [5]) or for spectroscopic applications. In the latter case, with the developed high-frequency gyro TWTs (see, for example, Ref. [22]), it is possible to increase the measurement sensitivity, providing a significantly higher signal-to-noise ratio compared with sources based on optical rectification of laser pulses. Notably, also, for the reduction of the required magnetic fields, electronic absorbers operating at cyclotron harmonics [15] may be implemented in the considered scheme. Thus, the experiments performed open a wide range of possibilities for the generation of coherent broadband radiation, which is potentially in demand for various applications.

Data that support the findings of this study are available from the corresponding author upon reasonable request.

ACKNOWLEDGMENTS

The work is supported by the IAP RAS Contract No. 0030-2021-0027 (Program "Development of equipment, technologies and research in the field of atomic energy use in the Russian Federation for the period up to 2024").

[1] H. J. Kim, E. A. Nanni, M. A. Shapiro, J. R. Sirigiri, P. P. Woskov, and R. J. Temkin, Amplification of Picosecond Pulses in a 140-GHz Gyrotron-Traveling Wave Tube, Phys. Rev. Lett. **105**, 135101 (2010).

[2] S. Alberti, F. Braunmueller, T. M. Tran, J. Genoud, J-Ph. Hogge, M. Q. Tran, and J-Ph. Ansermet, Nanosecond Pulses in a THz Gyrotron Oscillator Operating in a Mode-Locked Self-Consistent Q-Switch Regime, Phys. Rev. Lett. **111**, 205101 (2013).

[3] N. S. Ginzburg, A. M. Malkin, A. S. Sergeev, I. V. Zheleznov, I. V. Zotova, V. Y. Zaslavsky, G. S. Boltachev, K. A. Sharypov, S. A. Shunailov, M. R. Ul'masculov, and M. I. Yalandin, Generation of Subterahertz Superradiance Pulses Based on Excitation of a Surface Wave by Relativistic Electron Bunches Moving in Oversized Corrugated Waveguides, Phys. Rev. Lett. **117**, 204801 (2016).

[4] X. Lu, M. A. Shapiro, I. Mastovsky, R. J. Temkin, M. Conde, J. G. Power, J. Shao, E. E. Wisniewski, and C. Jing, Generation of High-Power, Reversed-Cherenkov Wakefield Radiation in a Metamaterial Structure, Phys. Rev. Lett. **122**, 014801 (2019).

[5] S. V. Kutsaev, B. Jacobson, A. Y. Smirnov, T. Campese, V. A. Dolgashev, V. Goncharik, M. Harrison, A. Murokh, E. Nanni, J. Picard, M. Ruelas, and S. C. Schaub, Nanosecond rf-Power Switch for Gyrotron-Driven Millimeter-Wave Accelerators, Phys. Rev. Appl. **11**, 034052 (2019).

[6] A. J. DeMaria, D. Stetser, and H. Heynau, Mode locked Nd glass, Appl. Phys. Lett. **8**, 174 (1966).

[7] T. Brabec, C. Spielmann, P. F. Curley, and F. Krausz, Kerr lens mode locking, Opt. Lett. **17**, 1292 (1992).

[8] T. Brabec and F. Krausz, Intense few-cycle laser fields: Frontiers of nonlinear optics, Rev. Mod. Phys. **72**, 545 (2000).

[9] U. Keller, Recent developments in compact ultrafast lasers, Nature **424**, 831 (2003).

[10] V. V. Lozhkarev, G. I. Freidman, V. N. Ginzburg, E. V. Katin, E. A. Khazanov, A. V. Kirsanov, G. A. Luchinin, A. N. Mal'shakov, M. A. Martyanov, O. V. Palashov, A. K. Poteomkin, A. M. Sergeev, A. A. Shaykin, and I. V. Yakovlev, Compact 0.56 petawatt laser system based on optical parametric chirped pulse amplification in KD*P crystals, Laser Phys. Lett. **4**, 421 (2007).

[11] E. V. Vanin, A. I. Korytin, A. M. Sergeev, D. Anderson, M. Lisak, and L. Vázquez, Dissipative optical solitons, Phys. Rev. A **49**, 2806 (1994).

[12] N. N. Rozanov, Dissipative optical solitons, Phys. Usp. **43**, 421 (2000).

[13] P. Grelu and N. Akhmediev, Dissipative solitons for mode-locked lasers, Nat. Photonics **6**, 84 (2012).

[14] N. S. Ginzburg, G. G. Denisov, M. N. Vilkov, I. V. Zotova, and A. S. Sergeev, Generation of "gigantic" ultra-short microwave pulses based on passive mode-locking effect in electron oscillators with saturable absorber in the feedback loop, Phys. Plasmas **23**, 050702 (2016).

[15] N. S. Ginzburg, G. G. Denisov, M. N. Vilkov, A. S. Sergeev, I. V. Zotova, S. V. Samsonov, and S. V. Mishakin, Generation of trains of ultrashort microwave pulses by two coupled helical gyro-TWTs operating in regimes of amplification and nonlinear absorption, Phys. Plasmas **24**, 023103 (2017).

[16] N. S. Ginzburg, E. R. Kocharovskaya, M. N. Vilkov, A. S. Sergeev, and S. E. Fil'Chenkov, Dissipative solitons in electron oscillators with a saturable absorber, Phys. Plasmas **25**, 093111 (2018).

[17] N. S. Ginzburg, G. G. Denisov, M. N. Vilkov, A. S. Sergeev, S. V. Samsonov, A. M. Malkin, and I. V. Zotova, Nonlinear Cyclotron Resonance Absorber for a Microwave Subnanosecond Pulse Generator Powered by a Helical-Waveguide Gyrotron Traveling-Wave Tube, Phys. Rev. Appl. **13**, 044033 (2020).

[18] A. V. Gaponov, M. I. Petelin, and V. K. Yulpatov, The induced radiation of excited classical oscillators and its use in high-frequency electronics, Radiophysics and Quantum Electronics **10**, 794 (1967).

[19] G. G. Denisov, V. L. Bratman, A. W. Cross, W. He, A. D. R. Phelps, K. Ronald, S. V. Samsonov, and C. G. Whyte, Gyrotron Traveling Wave Amplifier with a Helical Interaction Waveguide, Phys. Rev. Lett. **81**, 5680 (1998).

[20] V. L. Bratman, A. W. Cross, G. G. Denisov, W. He, A. D. R. Phelps, K. Ronald, S. V. Samsonov, C. G. Whyte, and A. R. Young, High-gain Wideband Gyrotron Traveling Wave Amplifier with a Helically Corrugated Waveguide, Phys. Rev. Lett. **84**, 2746 (2000).

[21] W. He, C. R. Donaldson, L. Zhang, K. Ronald, A. D. R. Phelps, and A. W. Cross, Broadband Amplification of Low-Terahertz Signals Using Axis-Encircling Electrons in a Helically Corrugated Interaction Region, Phys. Rev. Lett. **119**, 184801 (2017).

[22] W. He, L. Zhang, C. R. Donaldson, H. Yin, K. Ronald, A. W. Cross, and A. D. R. Phelps, The development of broadband millimeter-wave and terahertz gyro-TWA, Terahertz Science & Technology **13**, 90 (2020).

[23] N. S. Ginzburg, I. V. Zotova, A. S. Sergeev, V. Y. Zaslavsky, I. V. Zheleznov, S. V. Samsonov, and S. V. Mishakin, Mechanisms of amplification of ultrashort electromagnetic pulses in gyrotron traveling wave tube with helically corrugated waveguide, Phys. Plasmas **22**, 113111 (2015).

[24] G. G. Denisov, S. V. Samsonov, S. V. Mishakin, and A. A. Bogdashov, Microwave system for feeding and extracting power to and from a gyrotron traveling-wave tube through one window, IEEE Electron Device Lett. **35**, 789 (2014).

[25] Y. K. Chembo, D. Brunner, M. Jacquot, and L. Larger, Optoelectronic oscillators with time-delayed feedback, Rev. Mod. Phys. **91**, 035006 (2019).